Negative Differential Resistance in Transport through Organic Molecules on Silicon

Su Ying Quek,[1,*] J. B. Neaton,[2,†] Mark S. Hybertsen,[3,‡] Efthimios Kaxiras,[4,1,§] and Steven G. Louie[2,5]
[1]*Division of Engineering and Applied Sciences, Harvard University, Cambridge, Massachusetts, 02138, USA*
[2]*Molecular Foundry, Materials Sciences Division, Lawrence Berkeley National Laboratory, Berkeley, California 94720, USA*
[3]*Department of Applied Physics and Applied Mathematics and Center for Electron Transport in Molecular Nanostructures, Columbia University, New York, New York 10027, USA*
[4]*Department of Physics, Harvard University, Cambridge, Massachusetts, 02138, USA*
[5]*Department of Physics, University of California, Berkeley, California 94720, USA*

(Received 1 December 2006; published 8 February 2007)

Recent scanning tunneling microscopy studies of individual organic molecules on Si(001) reported negative differential resistance (NDR) above a critical applied field, observations explained by a resonant tunneling model proposed prior to the experiments. Here we use both density functional theory and a many-electron *GW* self-energy approach to quantitatively assess the viability of this mechanism in hybrid junctions with organic molecules on Si. For cyclopentene on *p*-type Si(001), the frontier energy levels are calculated to be independent of applied electric fields, ruling out the proposed mechanism for NDR. Guidelines for achieving NDR are developed and illustrated with two related molecules, aminocyclopentene and pyrroline.

DOI: 10.1103/PhysRevLett.98.066807 PACS numbers: 73.40.−c, 71.10.−w, 73.63.−b, 85.65.+h

Remarkable progress has been made of late in achieving atomic-scale control and characterization of organic molecules on silicon substrates with scanning-probe techniques [1–7]. These capabilities have provided the means for some of the most detailed studies of single-molecule conduction to date. Recent ultrahigh vacuum scanning tunneling microscopy (STM) studies of individual cyclopentene molecules on *p*-type hydrogen-free Si(001), a prototypical organic-silicon system, reported robust, reversible negative differential resistance (NDR) at 80 K, associated with a critical field of about 0.37 V/Å [8]; these results were explained by invoking the mechanism of resonant tunneling through a molecular state [9]. In contrast, room temperature STM studies [10] on *n*-type Si(001) observed hysteresis in the *I*-*V* characteristic and reported that NDR results from the desorption of cyclopentene molecules during measurement. Although the sample temperature and dopant type in the two studies differ, the contrasting conclusions have generated considerable debate over the origin of NDR observed in organic-molecule–Si systems.

Rakshit *et al.* [9] recently suggested that a semiconductor-molecule-metal junction can function as a resonant tunneling diode. Their model is summarized in Fig. 1. Consider a molecule bonded to a *p*-type semiconductor with a well-defined resonance positioned E_m below the Fermi energy E_F that is located at the Si valence band maximum (VBM) [Fig. 1(a)]. Initially, this level does not contribute to the current. However, a positive substrate bias causes the molecular level to move upward toward E_F. When the level eventually aligns with E_F, resonant tunneling through the molecular state occurs, resulting in a sharp increase in current [Fig. 1(b)]. A further increase in bias lifts the level into the band gap. This prohibits carrier flow through the molecular state, resulting in a drop in current and NDR [Fig. 1(c)].

Since the proposed NDR derives from intrinsic adsorbate levels, increased understanding of this mechanism would enable the tailoring of device transport properties through molecular design. However, for the above picture to hold at reasonable bias (applied electric field), three conditions must be satisfied: (1) The adsorbate must exhibit a well-defined resonance positioned E_m below E_F; (2) E_m must be small enough; and (3) the resonance should shift significantly with the applied field. Establishing the first two conditions requires quantifying the quasiparticle energy levels associated with the adsorbate. The final condition depends on the spatial distribution of the molecular orbital, which determines the effective voltage drop across the molecule. Previous calculations have treated both E_m and its evolution with applied field as adjustable parameters [11]. For cyclopentene on *p*-type Si(001), photoemission experiments were unable to resolve molecular resonances near E_F [12]. Quantitative calculations of energy levels require proper treatment of electron correlation effects that are not captured in density functional theory (DFT) [13–15].

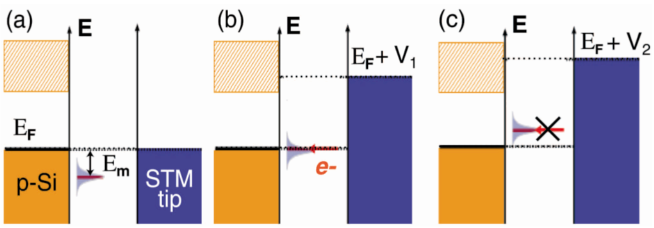

FIG. 1 (color online). Schematic depiction of resonant tunneling mechanism for NDR. (a) zero bias, (b) molecular level at resonance with E_F ($V\uparrow$, $I\uparrow$), (c) molecular level driven into Si band gap ($V\uparrow$, $I\downarrow$).

In this Letter, we employ a first-principles approach to characterize the molecular resonances (E_m and its field dependence) for representative organic molecules on Si(001). We find that the NDR reported in cyclopentene on p-type hydrogen-free Si(001) cannot result from resonant tunneling through intrinsic molecular states as previously proposed [8]. The cyclopentene frontier states with molecular character are strongly coupled to the Si substrate, and they neither form sharp resonances nor shift with applied electric field. However, with a slight modification of the molecule, localized molecular frontier orbitals can be introduced. For aminocyclopentene and pyrroline, calculations show that the frontier molecular resonances with N lone pair character can be driven into the Si band gap by applied electric fields. These examples show that by judicious design of the target molecule, a resonant tunneling mechanism for NDR in Si-based molecular junctions can be viable.

In our study, atomic and electronic structures are first determined within DFT, using the projector-augmented wave (PAW) method [16] and the local density approximation as implemented in the VASP code [17]. (Gradient corrections give similar results [18].) A positive substrate bias is simulated by the application of an external sawtooth potential normal to the Si surface (modeled here with a 6-layer Si slab passivated by H at the bottom). This field is largely screened inside the Si slab, but only partially by the molecular adsorbate. The resulting effective electric field across the molecule and vacuum region then corresponds to the field applied in the junction during the STM experiments. The applied field dependence of the electronic structure, derived from the change in self-consistent potential on the molecule, should be accurate in DFT. The zero-field E_m, initially obtained from DFT orbital energies, is then corrected by calculations of electron self-energies using many-electron perturbation theory in the *GW* approximation, as implemented in the PARATEC code [13,19]. Details of our DFT and *GW* calculations (including appropriately converged numerical cutoffs) are reported in a previous publication [18]. Taken together, the DFT and *GW* results provide a complete picture of the position and electric field sensitivity of the electronic resonances for each molecule studied [20].

Three systems are considered in this Letter: (a) cyclopentene on clean Si(001) [Fig. 2(a)]; (b) aminocyclopentene on H-terminated Si(001) [Fig. 2(b)]; and (c) pyrroline on H-terminated Si(001) [Fig. 2(c)]. 0.5 ML coverage is used for all systems. Prior experimental [3–7] and theoretical [18,21–23] studies have established that cyclopentene chemisorbs by a cycloaddition mechanism: the C-C π bond is broken in exchange for two σ C-Si bonds. The *cis* structure in Fig. 2, with H atoms closest to Si residing on the same side of the molecule, is both kinetically and thermodynamically favored for coverages of ≤ 0.5 ML [18]. Furthermore, aminocyclopentene has been observed to bind to exposed Si dimers on a H-terminated Si(001) substrate, in a geometry similar to that of cyclopentene [24]. We extend this concept to pyrroline [Fig. 2(c)], which can also bind to Si(001) through the same cycloaddition mechanism [4].

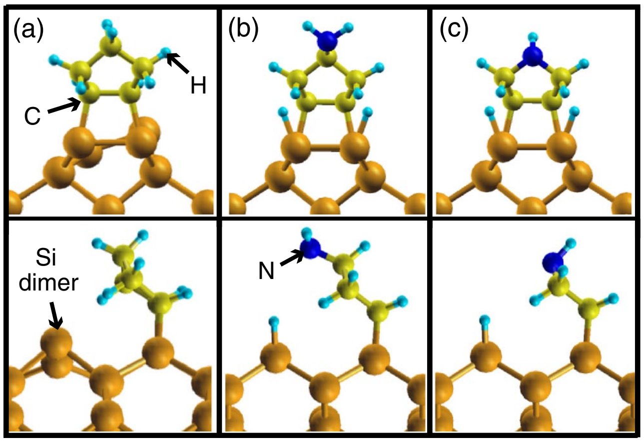

FIG. 2 (color online). Atomic structure of 0.5 ML (a) cyclopentene (C_5H_8) on clean Si(001), (b) amino-C_5H_8 on H-terminated Si(001), and (c) pyrroline on H-terminated Si(001). Orange (medium dark gray), green (medium gray), light blue (light gray), and dark blue (dark gray) circles represent Si, C, H, and N, respectively.

The projected densities of states (PDOS) on the molecules are shown in Figs. 3(a)–3(c), as derived from DFT energies. For all systems, there are no occupied surface states above the Si VBM [25], indicating that band bending is negligible at zero bias. For interpretation of STM experiments, tip-induced band bending is also negligible ($< \sim 0.2$ eV) in p-type Si(001) at positive sample bias [26]. For cyclopentene and pyrroline [Figs. 3(a) and 3(c)], significant broadening in the molecular PDOS suggests strong coupling of the frontier molecular states to Si states. In contrast, the aminocyclopentene PDOS [Fig. 3(b)] exhibits a sharp resonance at -1.5 eV. Further differences are elucidated by application of an electric field of 0.4 V/Å [Figs. 3(d)–3(f)]. The molecular resonance in

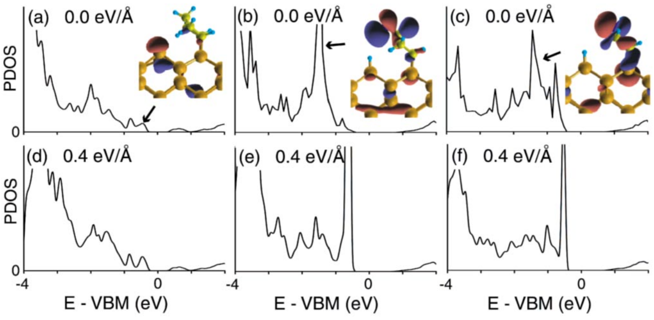

FIG. 3 (color online). LDA PDOS on the molecule for 0.5 ML C_5H_8 on clean Si(001) (a), (d), amino-C_5H_8 on H-terminated Si(001) (b), (e), and pyrroline on H-terminated Si(001) (c), (f). The insets show the orbitals associated with the leading states in each system. Pink (medium gray) and purple (dark gray) indicate positive and negative isocontours taken at the same value across all systems.

aminocyclopentene/Si junctions becomes sharper and increases in magnitude, shifting closer to the Si VBM [Fig. 3(e)]. This is in contrast to the cyclopentene PDOS, where the spectrum remains largely unchanged close to the VBM [Fig. 3(d)]. The pyrroline/Si junction is an interesting intermediate case. Although the molecular resonance close to the VBM has a width of about 1.5 eV at zero bias, the applied electric field sharpens this resonance considerably and moves it upward, toward the VBM [Fig. 3(f)]. Analysis of the frontier orbitals clarifies these results, as illustrated in the insets [Figs. 3(a)–3(c)]. The resonances in aminocyclopentene/Si and pyrroline/Si junctions are directly derived from the highest occupied orbital of the isolated molecules, localized on the N lone pairs. However, the broad frontier resonance for the cyclopentene/Si junction [-2.5 to 0 eV in Fig. 3(a)] is not identified with any specific orbital of the isolated molecule. Rather, these states correspond to C-Si and Si surface-related states that extend into bulk Si. This strong coupling to the substrate explains the relative lack of shift with field.

In Fig. 4, we plot E_m as a function of electric field by monitoring the leading feature in the molecular PDOS that comes closest to crossing the VBM with applied field. The leading state in the cyclopentene/Si junction is associated with the Si dimer and molecule ["dimer + molecule" state, Fig. 3(a)]. Its position relative to the Si VBM does not change with electric field, up to 1.3 V/Å [Fig. 4(a)]. In contrast, the leading state in aminocyclopentene, associated with the N lone pair [Fig. 3(b)], shifts linearly as a function of applied field, crossing the VBM at 0.7 V/Å [Fig. 4(b)]. In pyrroline, the leading state is also derived from the N lone pair [Fig. 3(c)], but the PDOS peak is broadened at fields ≤ 0.4 V/Å. In this case, we assign a single energy to the broadened resonance by performing a weighted average of the N-projected states contributing to the resonance [27]. The resulting average energy level also shifts approximately linearly with applied field, crossing the VBM at 1.0 V/Å [Fig. 4(c)]. We note here that the cyclopentene/Si and aminocyclopentene/Si geometries do not change significantly with the applied fields. Small structural distortions in the pyrroline/Si junction have negligible effect on the lone pair derived levels at all fields considered.

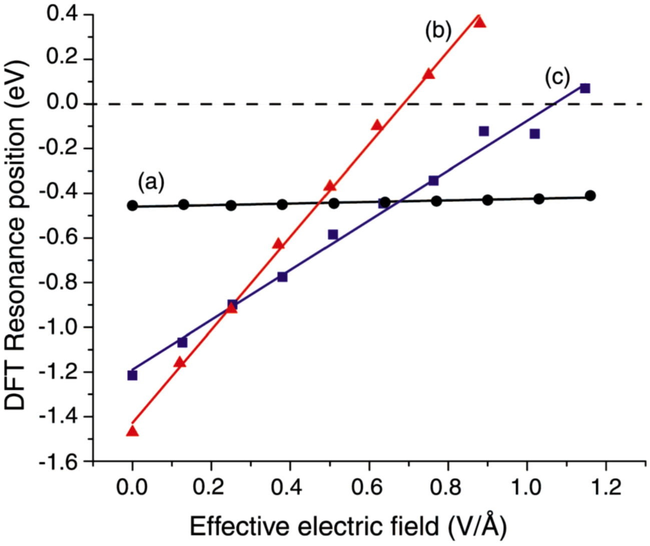

FIG. 4 (color online). DFT E_m as a function of the effective electric field. (a) 'dimer + molecule' state in C_5H_8/Si (black circles), (b) lone pair state in amino-C_5H_8/Si (red triangles), and (c) lone pair derived level in pyrroline/Si (blue squares). Straight lines of best fit are plotted in each case.

While the electric field dependence of the level position (the slope in Fig. 4) should be accurately given by DFT, we find that *GW* self-energy corrections shift the zero bias levels of the leading states further away from the Si VBM by as much as 90%. This trend is also observed for other molecular states. Our results are summarized in Table I, where DFT and *GW* E_m's for leading states in all three systems are listed with the rate of change in E_m with effective electric field F.

The implications of our results for the three prototype systems (Table I) are clear. First, the lack of a molecule derived resonance for cyclopentene near the Si VBM results in essentially no shift of the frontier states with applied field. As a result, the proposed intrinsic mechanism for NDR cannot apply. Second, field-induced movement of frontier molecular levels in aminocyclopentene/Si and pyrroline/Si junctions stems from their considerable weight on the molecular adsorbate. Third, the field dependence of the leading state in aminocyclopentene/Si junction is approximately twice that of the one in pyrroline/Si; the N lone pair in aminocyclopentene is further from the Si substrate than in pyrroline. Fourth, the critical field for the frontier level to cross the Si VBM is relatively large, even in these examples. Based on the DFT values of E_m, the critical fields are 0.7 and 1.1 V/Å for aminocyclopentene and pyrroline, respectively. Fifth, the *GW* corrections to E_m are substantial. They increase the estimates of the critical field significantly, to 1.4 and 1.8 V/Å, respectively.

In view of the experimental results for the cyclopentene/Si junction, we also studied systems at reduced coverage (0.125 ML) and with different contact geometries, including the *trans* configuration [18,23]; systems with a single C-Si bond per molecule and systems retaining the C=C bond were also examined. Boron ad-dimers and substitu-

TABLE I. Summary of results: DFT (within the LDA) and *GW* energies of leading states relative to the Si VBM (lone pair derived level in pyrroline); dE_m/dF is the rate at which the leading state is driven into the Si band gap by the effective field F (slope of best fit straight line in Fig. 4).

Molecule on Si	DFT E_m (eV)	*GW* E_m (eV)	dE_m/dF[eV/(eV/Å)]
C_5H_8	-0.5	-1.1	0.0
Amino-C_5H_8	-1.5	-2.9	2.1
Pyrroline	-1.2	-2.0	1.1

tional B dopants (immediately beneath the molecule, in subsurface layers, and away from the molecule in an 8-layered slab) were also considered, including the $c(4 \times 4)$ B surface structures discussed in [28]. Further details will be published elsewhere [27]. Our results indicate that none of these other structures have molecular states which cross the VBM at the critical field. An independent experimental study [10] of the cyclopentene/Si junction reported molecular desorption under moderate bias at room temperature on n-type substrates. For cyclopentene on p-type Si at 80 K, electron-simulated desorption was also reported, but at fairly low rates [29]. However, the lack of hysteresis in the I-V characteristic reported in Ref. [8] suggests that molecular desorption may not explain NDR in that case. Furthermore, the existence of a critical field also renders unlikely other NDR mechanisms that require a critical voltage, such as level crossing with localized tip states or electron-simulated desorption [29], for example. The origin of the NDR observed in [8] thus remains an interesting open question.

Our results allow us to develop some considerations that are important for achieving resonant tunneling NDR at lower fields. First, the rate at which a molecular state moves towards the VBM can be increased if its wave function is predominantly localized in a region that experiences a larger field-induced voltage drop relative to the substrate. Furthermore, such localization should reduce the coupling between this orbital and the Si electrode. If coupling to the other electrode is even weaker (e.g., for an STM tip), this can increase the ratio of peak to valley current, thus sharpening the NDR feature. Along these lines, promising molecular designs include the use of long, stiff backbones or fused rings, together with an amine group at the far end of the molecule away from the molecule-substrate interface. Second, for the molecules considered here, the N lone pair states are aligned closer to the Si VBM than intrinsic molecular states associated with σ bonds. This is related to the fact that the energy levels of N lone pair states in the gas-phase molecules are shallow compared with σ states. By designing molecules with shallow levels, the initial E_m will be closer to the VBM, enhancing the opportunity to achieve resonant tunneling. Third, increasing the work function of the electrodes (e.g., the substrate) may also lead to systems with intrinsic molecular states aligned closer to E_F. Possible future directions to pursue include using a semiconducting substrate with a larger work function than Si, or Si nanowires to take advantage of the increased work function due to quantum confinement.

This research was partially supported by NSF under No. DMR-0551195 and No. DMR04-39768, and the Nanoscale Science and Engineering Initiative under No. CHE-0117752. Work at the Molecular Foundry was supported by the Director, Office of Science, Office of Basic Energy Sciences, Division of Materials Sciences and Engineering, of the U.S. DOE under No. DE-AC02-05CH11231. S. Y. Q. and M. S. H. acknowledge support from A-STAR and NYSTAR, respectively. Computational resources were provided by NERSC and NPACI.

---

[*] Present address: Molecular Foundry, Materials Sciences Division, Lawrence Berkeley National Laboratory, Berkeley, California 94720, USA.

[†] Electronic address: JBNeaton@lbl.gov

[‡] Present address: Center for Functional Nanomaterials, Brookhaven National Laboratory, Upton, New York 11973, USA.

[§] Electronic address: kaxiras@physics.harvard.edu

[1] G. P. Lopinski, D. D. M. Wayner, and R. A. Wolkow, Nature (London) **406**, 48 (2000).
[2] J. L. Pitters *et al.*, J. Phys. Chem. B **110**, 2159 (2006).
[3] R. J. Hamers, J. Hovis, and H. Liu, Acta Phys. Pol. A **93**, 289 (1998).
[4] J. S. Hovis *et al.*, J. Vac. Sci. Technol. B **15**, 1153 (1997).
[5] J. S. Hovis, H. Liu, and R. J. Hamers, Surf. Sci. **404**, 1 (1998).
[6] J. S. Hovis, H. Liu, and R. J. Hamers, Appl. Phys. A **66**, S553 (1998).
[7] H. B. Liu and R. J. Hamers, Surf. Sci. **416**, 354 (1998).
[8] N. P. Guisinger, N. L. Yoder, and M. C. Hersam, Proc. Natl. Acad. Sci. U.S.A. **102**, 8838 (2005).
[9] T. Rakshit *et al.*, Nano Lett. **4**, 1803 (2004).
[10] J. L. Pitters and R. A. Wolkow, Nano Lett. **6**, 390 (2006).
[11] T. Rakshit, G. C. Liang, A. W. Ghosh, M. C. Hersam, and S. Datta, Phys. Rev. B **72**, 125305 (2005).
[12] S. Machida *et al.*, J. Phys. Chem. B **106**, 1691 (2002).
[13] M. S. Hybertsen and S. G. Louie, Phys. Rev. B **34**, 5390 (1986).
[14] W. G. Aulbur, L. Jonsson, and J. W. Wilkins, in *Solid State Physics*, edited by H. Ehrenreich (Academic Press, Orlando, 2000), p. 1.
[15] J. B. Neaton, M. S. Hybertsen, and S. G. Louie, Phys. Rev. Lett. **97**, 216405 (2006).
[16] P. E. Blochl, Phys. Rev. B **50**, 17 953 (1994).
[17] G. Kresse and J. Furthmuller, Phys. Rev. B **54**, 11 169 (1996).
[18] S. Y. Quek *et al.*, Phys. Status Solidi (b) **243**, 2048 (2006).
[19] M. S. Hybertsen and S. G. Louie, Phys. Rev. Lett. **55**, 1418 (1985).
[20] Current-induced forces or level shifts are neglected, an acceptable approximation for the low current regime in the STM experiments (current ~nA, conductance $\sim 10^{-5}$ G_0).
[21] K. Akagi *et al.*, Appl. Surf. Sci. **234**, 162 (2004).
[22] J. H. Cho and L. Kleinman, Phys. Rev. B **64**, 235420 (2001).
[23] W. Lu, W. G. Schmidt, and J. Bernholc, Phys. Rev. B **68**, 115327 (2003).
[24] Z. Lin *et al.*, Langmuir **18**, 788 (2002).
[25] The Si VBM is obtained by aligning the average potential in the Si slab with that in bulk Si.
[26] M. McEllistrem, G. Haase, D. Chen, and R. J. Hamers, Phys. Rev. Lett. **70**, 2471 (1993).
[27] S. Y. Quek *et al.* (to be published).
[28] M. Ramamoorthy, E. L. Briggs, and J. Bernholc, Phys. Rev. B **59**, 4813 (1999).
[29] N. L. Yoder *et al.*, Phys. Rev. Lett. **97**, 187601 (2006).